

STRUCTURAL AND AEROELASTIC OPTIMIZATION OF A LARGE AIRCRAFT WING WITH A PASSIVE TWIST WINGTIP

Yingjun Pan¹, Mushfiqul Alam¹, Andrea Spinelli² & Estela Bragado Aldana¹

¹Centre for Aeronautics, School of Aerospace, Transport & Manufacturing, Cranfield University, Bedford, UK ²Centre for Propulsion and Thermal Power, School of Aerospace, Transport & Manufacturing, Cranfield University, Bedford, UK

Abstract

A flexible toolset for structural and aeroelastic analysis is needed for the multi-disciplinary optimization of an overall aircraft design. This paper presents the use of multi-fidelity structural analysis and aeroelastic tailoring tools in designing an optimized composite wing for a large aircraft. The optimization of the composite wing structure is divided into two stages, adhering to multiple design constraints. The first stage focuses on minimizing the wing structural weight subject to static strength and aeroelastic constraints, utilizing the in-house Structural Layout Tool (SLoT) and Structural Analysis Tool (SAIT) that relies on skin-stringer panels and wingbox elements developed at Cranfield University. Here, the skin-stringer panel sizing, including skin thickness, web thickness, and stringer sizing, are used as design variables. The second stage involves aeroelastic tailoring, where skin and spar laminate layups are modified using a high-fidelity FE-based optimization program that integrates NASTRAN, SLoT-SAIT toolset, and a MATLAB optimizer. This aims to maximize the flutter speed for the intended wing design. Furthermore, this study explores the incorporation of a Passive Twist Wingtip (PTWT) in the wing design as an additional module within the toolset framework. The PTWT design has a specific length and shaft location, and it replaces the fixed wingtip of the FE model built in the SLoT-SAIT optimization stages. This PTWT module chooses torque spring stiffness and mass as design variables, focusing on flutter suppression in the initial design. Overall, this paper demonstrates that using the design and optimization of the current multi-fidelity toolset not only achieves weight optimization but also produces advantageous aeroelastic characteristics, particularly in terms of flutter speed improvement for large aircraft.

Keywords: wing structure, aeroelastic tailoring, flutter, passive twist wingtip

Nomenclature

MDO Multi-Disciplinary Optimization

PTWT Passive Twist Wingtip
CRM Common Research Model
DPW Drag Prediction Workshop
FEM Finite Element Models
SLoT Structural Layout Tool
SAIT Structural Analysis Tool

FI Failure Index

1. Introduction

In the context of future development for large commercial aircraft, improving design and optimization methodologies is crucial to meet environmental challenges such as significant reductions in noise, CO₂ emissions, and fuel consumption [1, 2]. A key focus in aviation is shortening the development timeline for new configurations and technologies. Additionally, it is essential to comprehensively

assess new technologies, taking into account all relevant disciplines and their interactions from an overall aircraft perspective. The use of multi-fidelity analysis toolsets and Multi-Disciplinary Optimization (MDO) for aircraft design offers wide-ranging applicability and accelerates the derivation of design options and assessments. This signifies a paradigm shift towards potential configurations and enhanced efficiency in the future. Furthermore, the integration of advancements in materials and structures with aerodynamic technologies is crucial for improving aircraft efficiency, which is determined by aerodynamic performance, specifically the lift-to-drag ratio, aircraft empty mass, and fuel consumption [3].

Designing and optimizing wings is a complex, multidisciplinary challenge within the field of airframe technology, necessitating careful consideration of practical design and manufacturing constraints. The incorporation of composite materials and large aspect ratio wings have notably advanced the aerodynamic efficiency of large aircraft. However, these high aspect ratio wings while being aerodynamically efficient are susceptible to increased flexibility issues leading to challenges such as static deformation, aileron reversal, and aeroelastic instability [4]. These issues necessitate consideration in the initial stages of the aircraft design process. Therefore, an effective method for integrating structural and aeroelastic analyses of aircraft is required. Concerning composite wings, aeroelastic tailoring techniques have emerged as a pivotal optimization strategy [5, 6, 7]. This approach adapts the strategic alignment of fiber directions to internal loads, thereby mitigating dynamic aeroelastic responses. Such optimization results in wings that are not only lightweight but also exhibit enhanced strain tolerance under the aeroelastic constraint.

On the other hand, lightweight flexible aircraft present challenges of increased aerodynamic loading when subject to external disturbances such as gusts which can lead to structural failure, compromised aeroelastic stability, and reduced flight controllability [8]. This has necessitated the investigation of both active and passive load alleviation technologies alongside aircraft structural sizing in preliminary aircraft design. Passive gust alleviation devices, compared to active control technologies generally operated via wing leading or trailing edge control surfaces, are simpler, more reliable, and more effective in gust alleviation [9, 10]. A Passive Twist Wingtip (PTWT) design, features a distinct wing segment attached at the wingtip via a shaft and torque spring connected to the front spar of the wing [11]. With the shaft positioned ahead of the aerodynamic center, the gust-induced aerodynamic force will cause a nose-down twist in the PTWT. This leads to a negative angle of attack and a subsequent negative aerodynamic force on the PTWT, thereby reducing the load on the wing. The effectiveness of this design in reducing gust responses and flutter suppression has been validated through previous studies on a 200-seater airliner [11] and flying wing aircraft [12].

The aim of our project is to develop an efficient and comprehensive flexible toolset that integrates structural and aeroelastic analyses with PTWT technology. This toolset is used to evaluate the preliminary design of composite wings for large aircraft. It incorporates multi-fidelity methods, combining numerical analysis with finite element model-based analysis, to achieve better industry oriented solutions with an acceptable level of accuracy and practical optimization approaches. The NASA Common Research Model (CRM), which features a wing-body-tail configuration characteristic of modern wide-body, long-range aircraft, is utilized in this paper to demonstrate the design, analysis, and optimization technologies [13]. Since the inception of the Drag Prediction Workshop (DPW) series, the CRM has been extensively used as a test case for applied computational aerodynamics, focusing on CFD verification and validation alongside wind-tunnel testing for aerodynamic shape optimization [14, 15, 16, 17]. Additionally, recent interest has emerged in employing the CRM configuration for structural design and static aeroelastic analysis [18, 19, 20]. Currently, two primary Finite Element Models (FEMs) for CRM, V12 and V15, are under discussion [21]. V12 employs a three-spar wingbox architecture designed to assess stress and buckling, while V15 utilizes a two-spar wingbox architecture to enhance aeroelastic meshing efficiency and optimization. Building on conventional designs, this study expedites the development of a detailed baseline wingbox model that meets material failure, buckling, and manufacturing constraints, utilizing the latest DPW-7 configuration and loading data [22]. Our in-house programs, the Structural Layout Tool (SLoT) and Structural Analysis Tool (SAIT), facilitate structural weight savings by optimizing the sizing of components (skins, spars, and stringers) and tailoring the laminate layup. These adjustments help mitigate gust response and

increase the maximum flutter speed through the user of a high-fidelity FEM.

The paper is structured as follows: Section 2.outlines the medium-fidelity toolset methodology and optimization methods. Section 3describes the design and analysis of a baseline wingbox model using the SLoT-SAIT toolset, achieving an optimized wing design with reduced weight. Section 4.demonstrates aeroelastic tailoring for the optimized wing to achieve an increased flutter speed through the integration of the SLoT-SAIT toolset and NASTRAN. Section 5. explores the implementation of a PTWT design to further enhance flutter characteristics, concluding with final remarks in Section 6.

2. Multi-Fidelity Toolset Architecture and Optimization Method

2.1 Multi-Fidelity Toolset for Preliminary Design

For an overall aircraft design, the developed multi-fidelity toolset for wing structural and aeroelastic optimization, encompasses three levels of structural model fidelity, as shown in Figure 1. The low-fidelity model (Module 3), typically a beam model or a discrete beam assembly, aligns with numerical and test data at 'discrete' points. It predicts static and dynamic behaviors of wings in conceptual design, approximating deflection and dynamic response but lacks detailed buckling, stress, and strain analyses for strength evaluation.

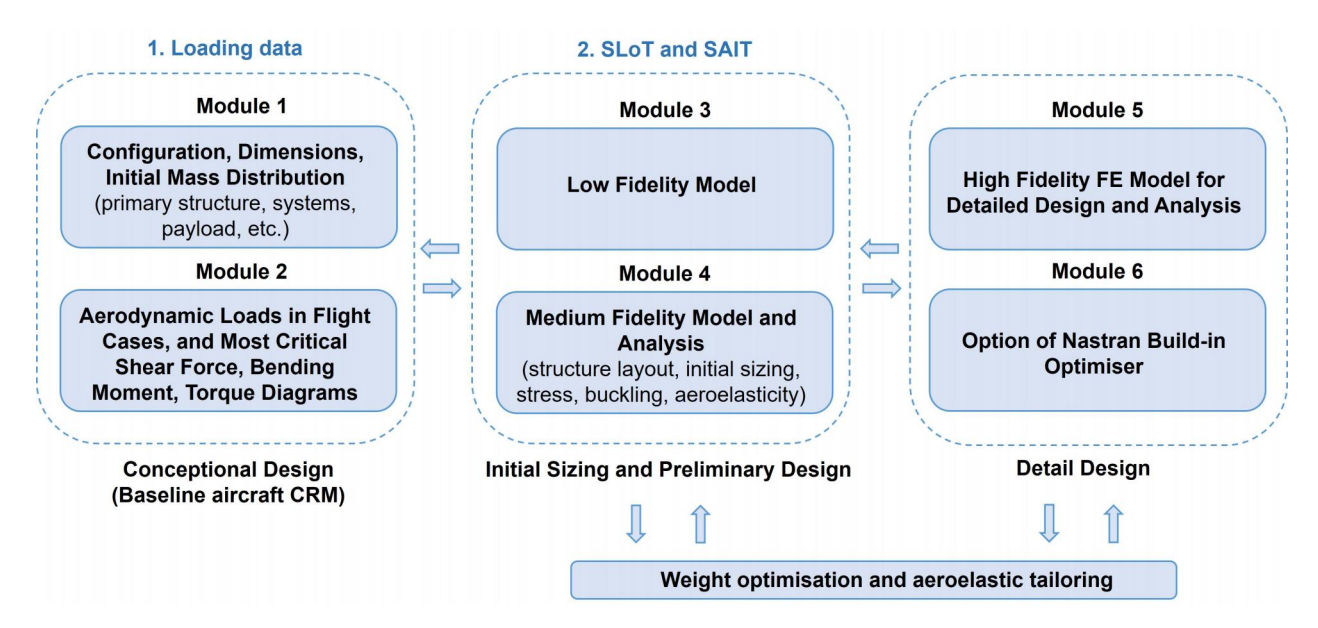


Figure 1 – Architecture of the multi-fidelity toolset for wing structural and aeroelastic optimization.

The medium fidelity model (Module 4), representing a semi-monocoque box structure with stiffened thin-walled panels, more accurately depicts the stiffness and mass distribution of a wing by modeling key structural components, including spar webs and flanges, skin, and stiffeners. It produces detailed predictions of buckling, stress, and strain results for each component, though with limited detail at the element level (refined local region). It also enables laminate analysis for composite components, facilitating layup optimization under buckling, strength, and aeroelastic constraints. Its results, providing detailed component sizing, bridge the gap between low-fidelity and high-fidelity FE models.

Modules 3 and 4, designed as in-house modular computational programs at Cranfield University, i.e., SLoT and SAIT, facilitate interactive MDO to expedite the generation and assessment of airframe design options. The high-fidelity model (Modules 5 and 6) uses commercial software NASTRAN for detailed stress and strain analyses at the element level. Additionally, a gradient-based optimizer in Matlab is integrated into the toolset for wing optimization, focusing on weight reduction and aeroelastic behavior improvement. These multi-fidelity modules (3 to 6) collectively form a preliminary airframe design package. In future project development, this package will be integrated into PDOPT, an MDO-based probabilistic machine-learning model, to identify promising design space areas based on user requirements and select optimal configurations for further aircraft development [23].

2.2 Weight Optimization and Aeroelastic Tailoring

A preliminary design of a composite wing that minimizes weight while meeting static strength, buckling, and aeroelastic constraints is performed, as shown in Figure 2. Targeted at weight reduction, design variables such as skin thickness, web thickness, and initial stringer sizing are optimized in the SLoT stage based on load analysis data. It produces initial skin-stringer panel sizing under stress constraints of Failure Index (FI) and critical strain for damage tolerance. The SAIT is then employed to calculate the bending and torsional stiffness of wingbox elements and to perform aeroelastic analysis, ensuring the flutter speed meets airworthiness requirements.

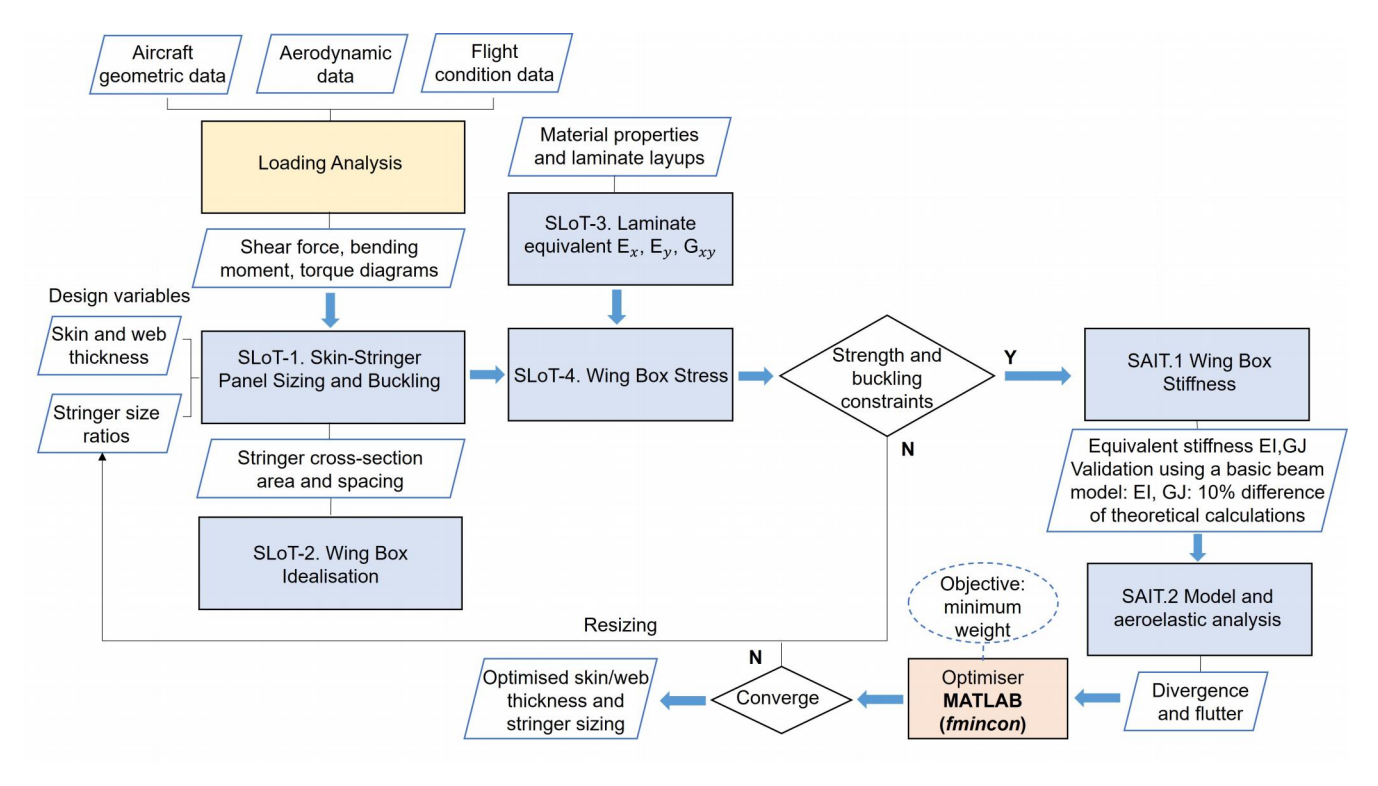


Figure 2 – Flow chart of SLoT-SAIT toolset for wing weight optimization.

Following the optimized sizing of structural components, a secondary optimization focuses on the laminate layups of the composite skin and spar webs, with the objective of maximizing flutter speed within the constraints of the specified wing weight. Figure 3 illustrates the integration of SLoT and SAIT programs with the high-fidelity FEM, using the same wingbox geometry. The equivalent laminate properties (E_x , E_y , and G_{xy}) of the composite panels serve as inputs for NASTRAN to perform detailed stress, buckling, free vibration, and aeroelastic analyses.

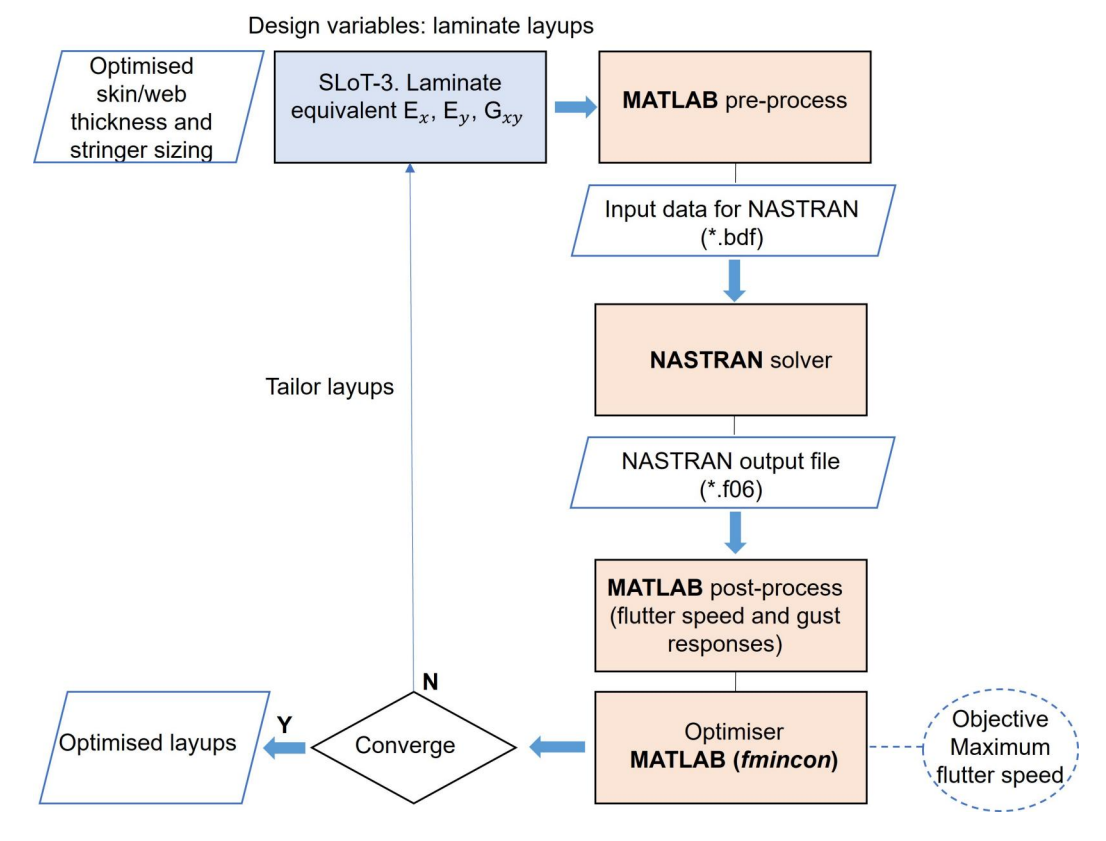


Figure 3 – Flow chart of wing aerodynamic tailoring.

The optimization program referenced in Figure 2 and Figure 3 utilizes the MATLAB function 'fmincon', a gradient-based optimizer, following the outlined equation [24]:

$$\min_{x} f(x) \text{ such that} \begin{cases} c(x) \leq 0, \\ ceq(x) = 0, \\ A \cdot x \leq b, \\ Aeq \cdot x = beq, \\ lb \leq x \leq ub. \end{cases} \tag{1}$$

here f(x) is the function to be minimized; c(x), ceq(x) are nonlinear constraint functions; A, Aeq are linear constraint functions; and lb, ub define the lower and upper bounds on the variables.

3. Composite Wing Structural Optimization

3.1 Aircraft Data and Structural Layout

Essential design data of CRM are detailed in Table 1. Figure 4 displays the planform views of the CRM FEM V15 [21] on the left side and the baseline wingbox model created in this study on the right side. The baseline wingbox model consists of an inner wingbox with ribs aligned in the flight direction and an outer wingbox with ribs perpendicular to the front spar. The front and rear spars of the outer wingbox are located at 11% and 70% of the local chord lengths, respectively. The front, middle and rear spars of the inner wingbox are located at 10%, 31%, and 70% of the local chord lengths, respectively. The wing structure layout is divided into 7 sections from the wingtip to root shown in Figure 5.

Table 1 – Aircraft technical data.

Wing aspect ratio	9.00	Maximum takeoff weight (kg)	298,000
Wing area (m ²) (including left wing)	383.65	Engine mass (kg)	6,218
Wing semi-span (m)	29.38	Operational empty weight (kg)	138,100
Mean chord (m)	7.01	Cruise speed (m/s)	289
Quarter-chord sweep angle (°)	35	Cruise lift coefficient	0.5

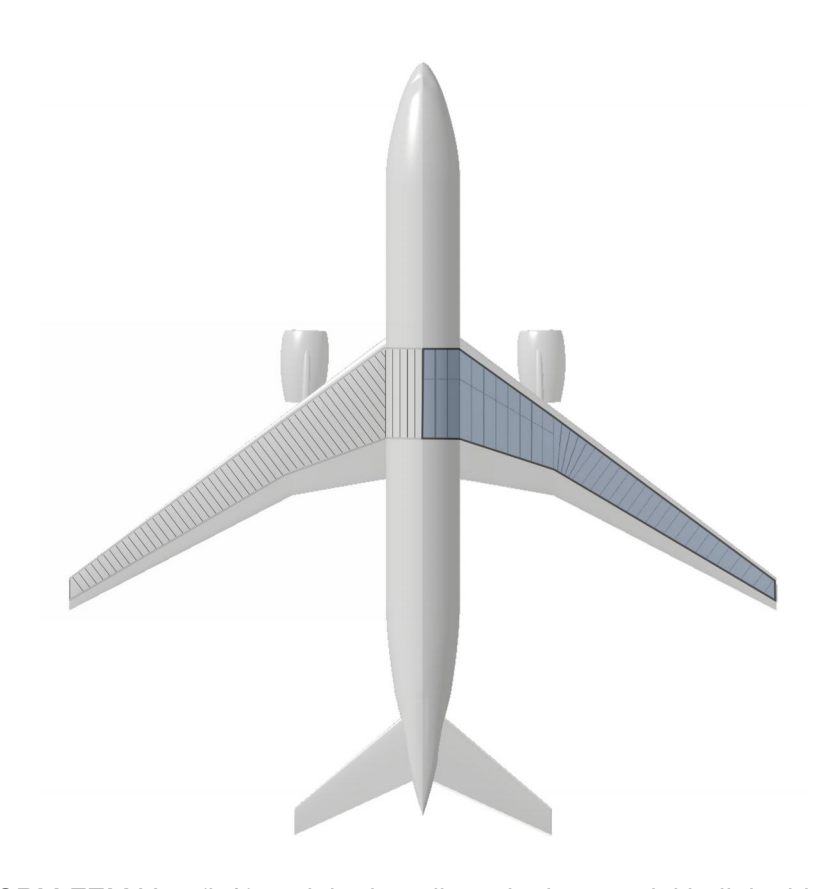


Figure 4 – CRM FEM V15 (left) and the baseline wingbox model built in this study (right).

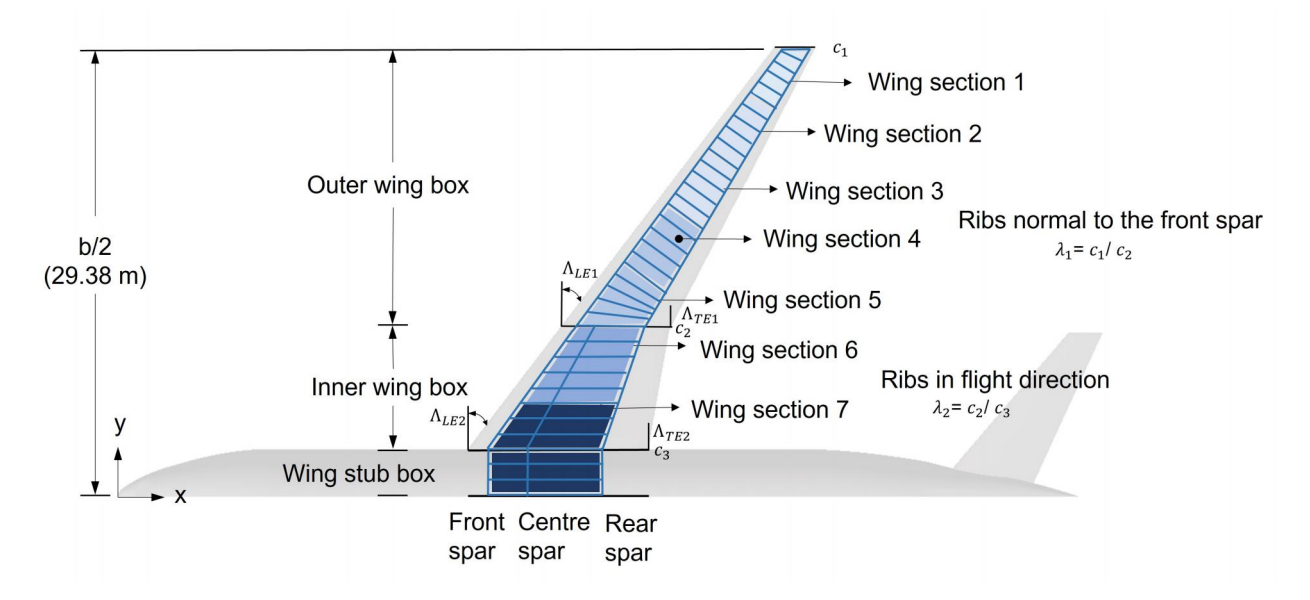


Figure 5 – Wingbox regions.

3.2 Design and Analysis of the Baseline Wingbox Model

A summary of the material properties employed in modeling the wing is provided in Table 2. An intermediate modulus carbon/epoxy composite prepreg has been selected for panel elements (skin and webs), characterized by material properties including modulus E_1 and strength X_t and X_c in the fiber direction, E_2 , X_c and Y_c in the off-fiber direction and shear modulus G_{12} and strength S. The initial structural design is conducted using quasi-isotropic layups with ply percentages of (50/40/10), aligned with established design rules and manufacturing constraints [25].

Location	Material	Material Properties				
Spar caps, stringers, rib flange and web stiffeners	Aluminium	Density (kg/m³)	Е (Pa)	G (Pa)	v
(T-shape cross-section)		2700	7.0	e10	2.69e10	0.3
Skin covers, spar and rib	Composite material	Density (kg/m ³)	E_1 (Pa)	E ₂ (Pa)	G ₁₂ (Pa)	<i>v</i> ₁₂
webs	(M91/IM10 UD prepreg)	1586	1.76e11	1.58e10	5.6e9	0.27
		X_t 3.52e9	X _c (Pa) 1.88e9	Y _t (Pa) 4.27e7	Y _c (Pa) 1.27e8	S (Pa) 1.05e8

Table 2 – Material properties of the baseline wing

The 2.5 g symmetric pull-up maneuver load at sea level is critical for the design, analysis, and sizing optimization of the CRM wing structure [21]. This study rapidly calculates aerodynamic loads by using two different programs to ensure tool versatility and accuracy. These include the ESDU 95010 computer program [26] and an in-house loading computation program implemented in SLoT. For the initial structural design, the wing is divided into 33 boxes from tip to root according to rib positions and grouped into 7 sections with uniform skin and web thickness (Figure 5). A wingbox is idealized in SLoT as skin-stringer panels as shown in Figure 6. This example illustrates a double-cell box for the interior wing. The roles of stringers and skins are distinctly separated: skins are assumed to carry only shear loads, while their contribution to resisting direct stress is considered with the stringers as booms. Using input values for skin and web thickness and stringer size ratio, the wingbox with a swept and tapered stringer arrangement is modeled for stress and buckling analysis. The baseline sizing is established with a safety factor of 2, ensuring compliance with allowable strength. As a result, the thickness values of skin and web panels from wing sections 1 to 7 are provided in Table 3.

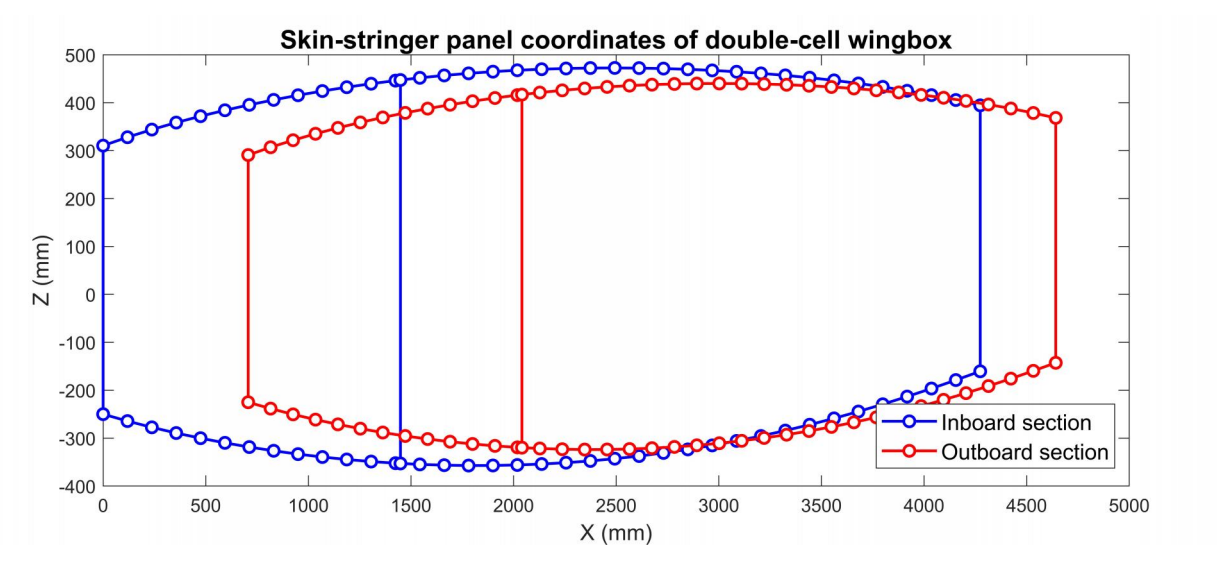


Figure 6 – Skin-stringer panel coordinates of a double-cell wingbox

Table 3 – Panel thickness of the baseline wing

Section No.	Skin (mm)	Front Spar (mm)	Rear Spar (mm)	Middle Spar (mm)
1	3.68	3.68	3.68	-
2	5.52	5.52	5.52	-
3	6.624	7.36	7.36	-
4	7.728	8.832	7.728	-
5	7.728	8.832	8.832	-
6	17.664	17.664	17.664	17.664
7	18.032	18.032	18.032	18.032

3.3 Weight Optimization Results

3.3.1 Optimizing Sizing and Weight

In order to lower the weight of the baseline wing to a desirable value, the panel sizing of each wingbox is further optimized by integrating the SAIT programs under the constraint of flutter speed (Figure 2). This step is carried out by using the optimizer settings compiled in Table 4. For the minimum weight optimization, the function value represents the total wingbox weight. A single-cell box of the outer wing has four variables: upper skin, lower skin, front spar, and rear spar. A double-cell box of the inner wing contains five variables, adding a middle spar to the list. Under the ultimate load, the upper boundary for FI is set to 1, and the maximum strain is limited to 3500 $\mu\varepsilon$. The lower boundary for flutter speed is set at $1.15V_D$ as required by CS-25, where V_D is the dive speed. Given the CRM dive speed of $185 \ m/s$ [27], the critical flutter speed is $212.75 \ m/s$.

Table 4 – Weight optimization settings for the baseline wing

Optimization objective	Minimize wing weight
Optimization variables	Skin and web thickness
Constraint 1: Maximum stress criterion FI	≤ 1
Constraint 2: Tsai-Wu criterion FI	≤ 1
Constraint 3: Allowable strain	\leq 3500 $\mu\varepsilon$
Constraint 4: Buckling factor	≥ 1
Constraint 5: Flutter speed	$\geq 1.15V_D$

By significantly reducing the number of design variables and independently calculating each wingbox, the optimization process can be completed in several minutes. Figure 7 shows the convergence history of the integrated MATLAB program, with the current point indicating the half values of the skin and web ply numbers. Besides, the optimized skin and web thicknesses and the total weight of each wing section, including stringer mass, are presented in Figure 8. It is noted that the inner wing features thicker laminates compared to the outer wing, attributed to the significantly higher shear forces near the wing root. The results demonstrate a 13.7 % reduction in the overall skin and spar weight of the wing, with a final value of 5867 kg.

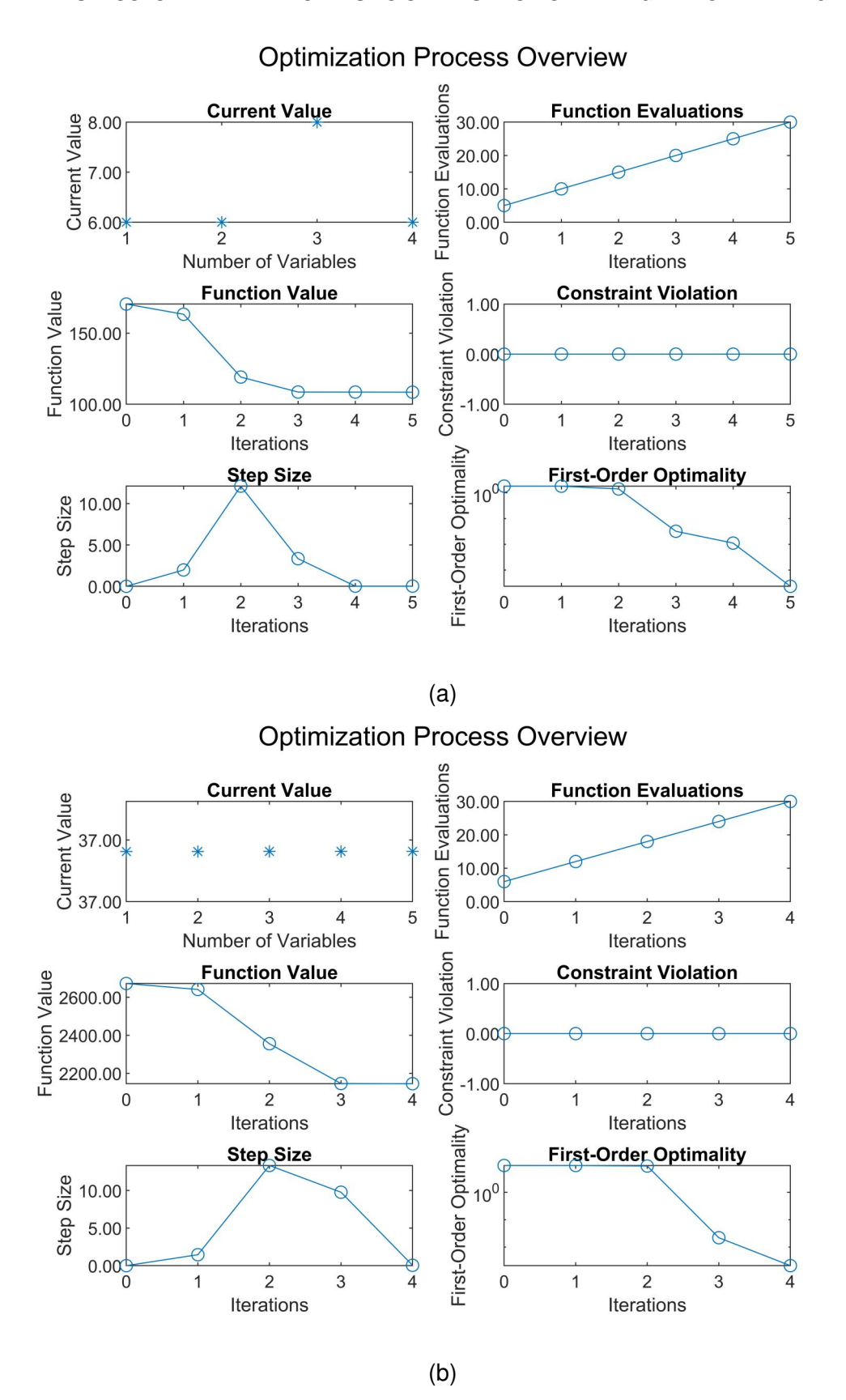


Figure 7 – Convergence history for weight optimization: (a) single-cell wingbox and (b) double-cell wingbox.

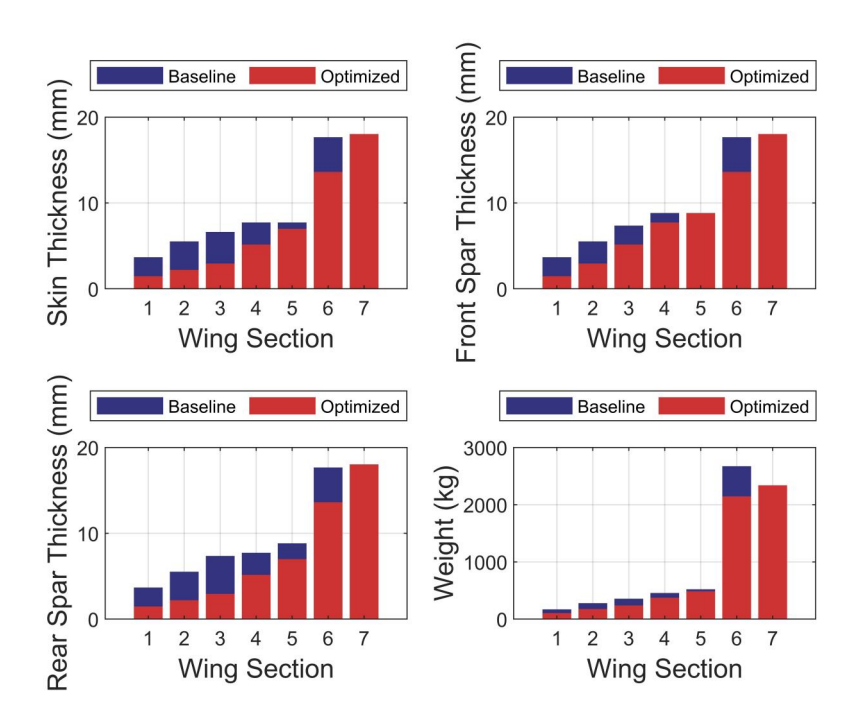


Figure 8 – Optimized sizing and weight of the baseline wing.

For each wingbox, the bending rigidity (EI), torsional rigidity (GJ), and bending-torsion coupling rigidity (CK) are calculated by the SAIT.1 program (Figure 2) based on geometry, material properties, and laminate layups. These stiffness values significantly impact flutter characteristics. Figure 11 presents the bending and torsional stiffness distributions for both the baseline and optimized wings. Due to reduced thickness, the optimized wing has lower stiffness values compared to the baseline wing. The SAIT.2 program (Figure 2) then computes flutter speeds based on the dynamic stiffness matrix method, resulting in 550.94 m/s for the baseline wing and 514.01 m/s for the optimized wing. Considering the engine in wing section 6 as a lumped mass, the wing has a flutter speed of 341.56 m/s, which is well above the critical flutter speed of 254 m/s, thus satisfying the airworthiness requirement.

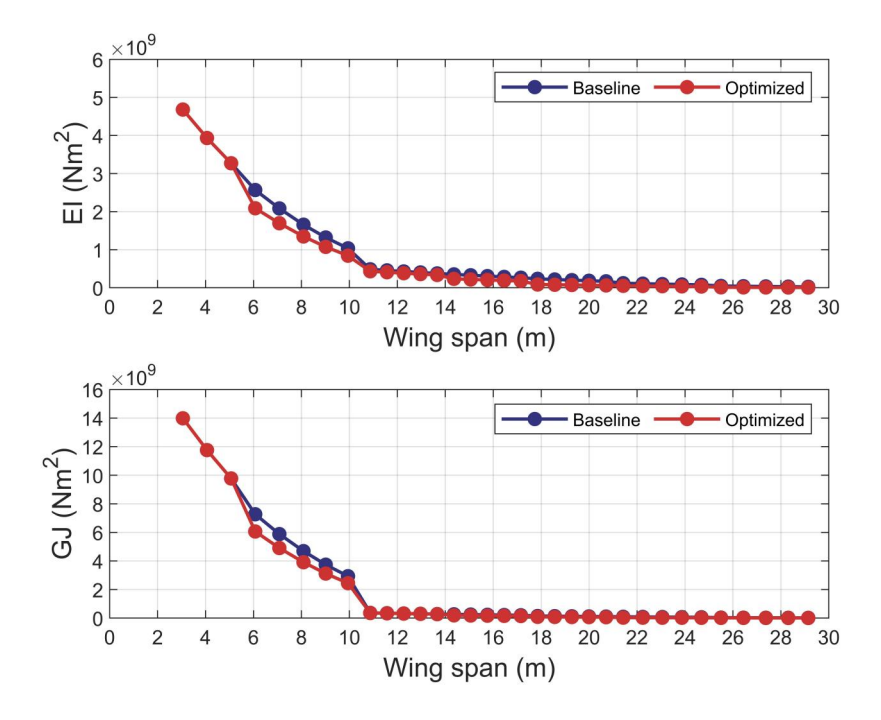


Figure 9 – Bending stiffness (top) and torsional stiffness (bottom) of the baseline wing and the optimized wing.

3.3.2 Detailed Analysis

Using the Nastran solver, the optimized wing based on the preliminary design from the SLoT-SAIT toolset is verified for stress, strain and flutter speed. The FE model is created with the same skin panel, spar, and stringer sizing obtained from the toolset. The total weight of the wing including ribs is 13,310 kg. As shown in Figure 10, the wingtip deflection is 0.29 m. Under the 2.5 g load factor, the maximum static stress and strain are 768 MPa and 514 $\mu\varepsilon$, respectively, both below the failure index and damage tolerance limits. The addition of ribs significantly enhances strength, indicating potential for further optimization in the detailed design phase.

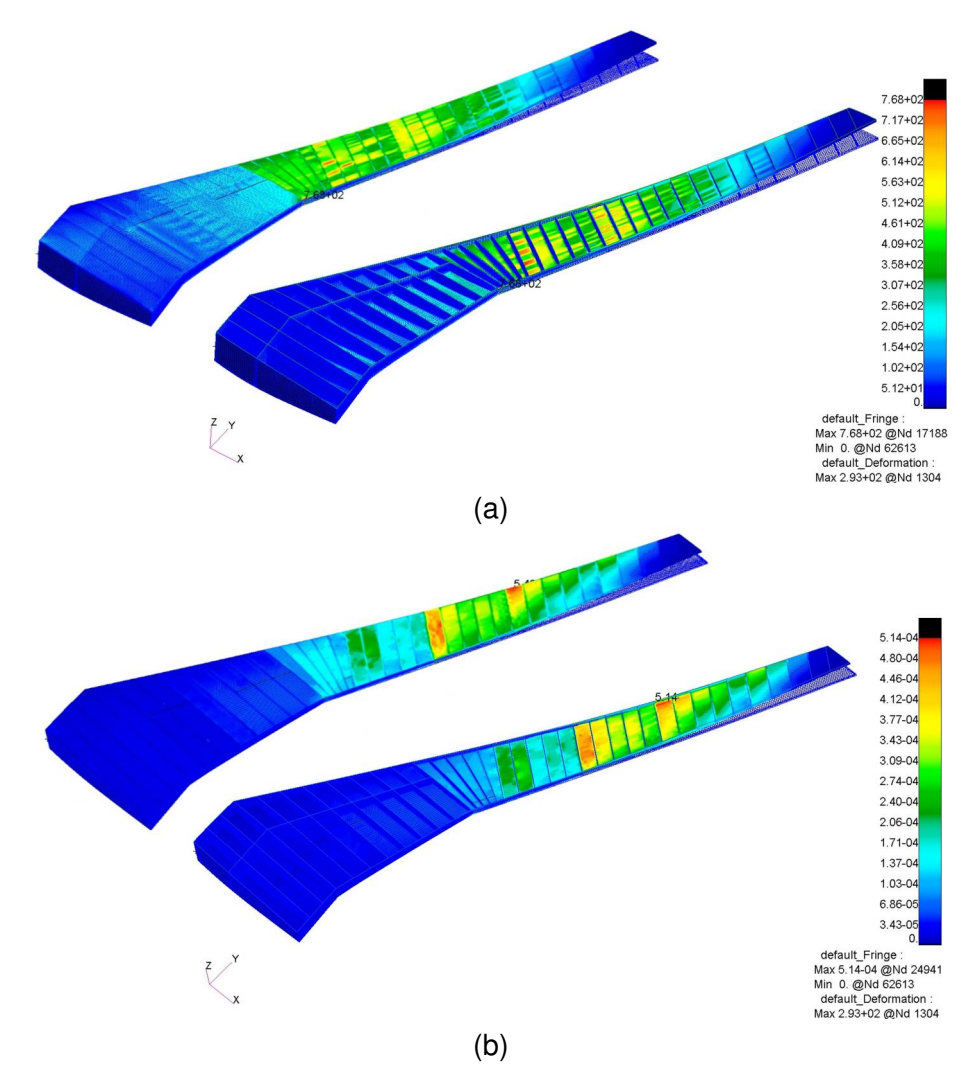


Figure 10 – Stress (a) and strain (b) of the optimized wing under the 2.5 g load.

For the flutter analysis, a modal analysis of the wing is conducted with the first six modes presented in Figure 11: 1^{st} bending $(6.05\,Hz)$, 2^{nd} bending $(19.28\,Hz)$, 3^{rd} bending $(24\,Hz)$, 4^{th} bending $(38.20\,Hz)$, 1^{st} torsion $(60.07\,Hz)$, and 2^{nd} torsion $(63\,Hz)$. The flutter results obtained by using the PK method are shown in Figure 12 as V-g and V-f plots. A flutter speed of 513.29 m/s and a frequency of 62 Hz are obtained when the damping reaches zero, which is well consistent with the flutter results of the SAIT.2 program. The coupling of the 1^{st} and 2^{nd} torsion modes is the most critical. These results demonstrate that the optimized wing structure has an adequate safety margin with weight savings.

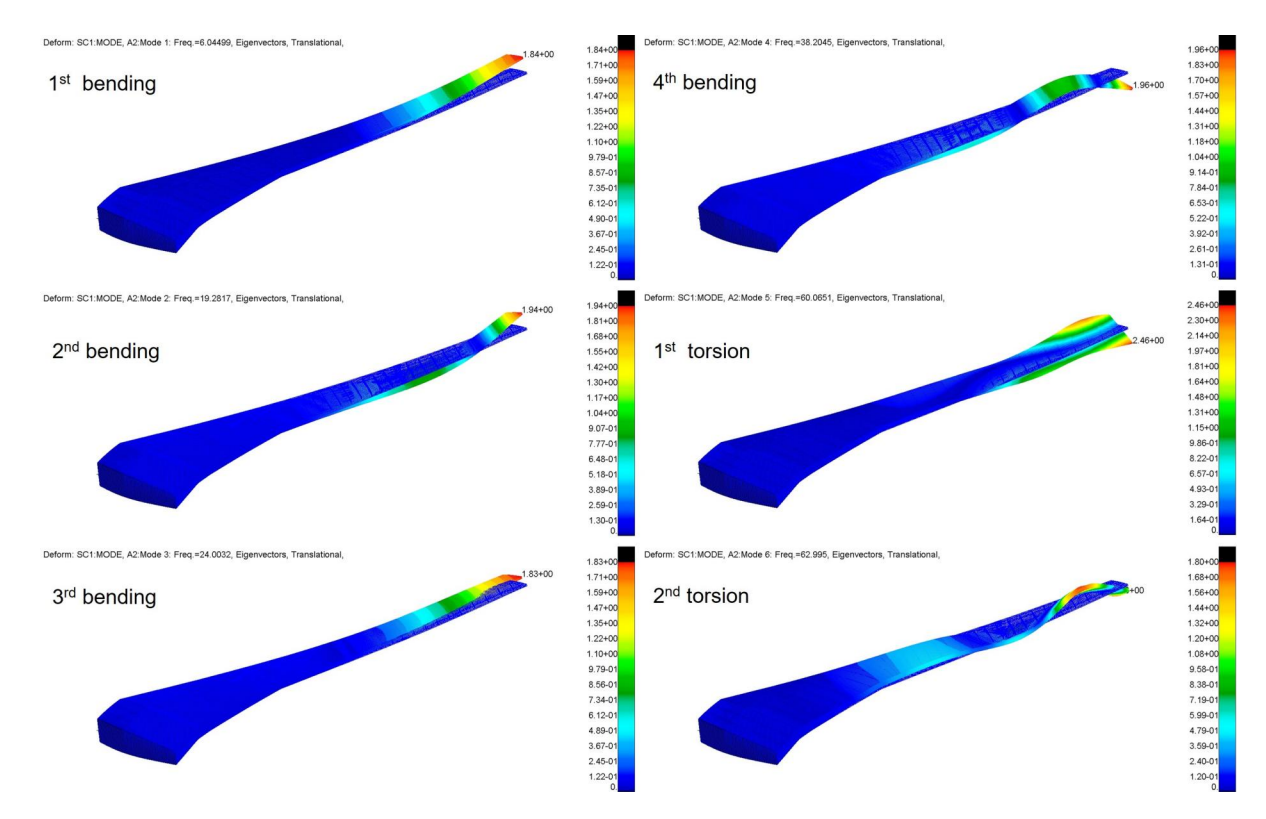


Figure 11 - Mode shapes of the optimized wing

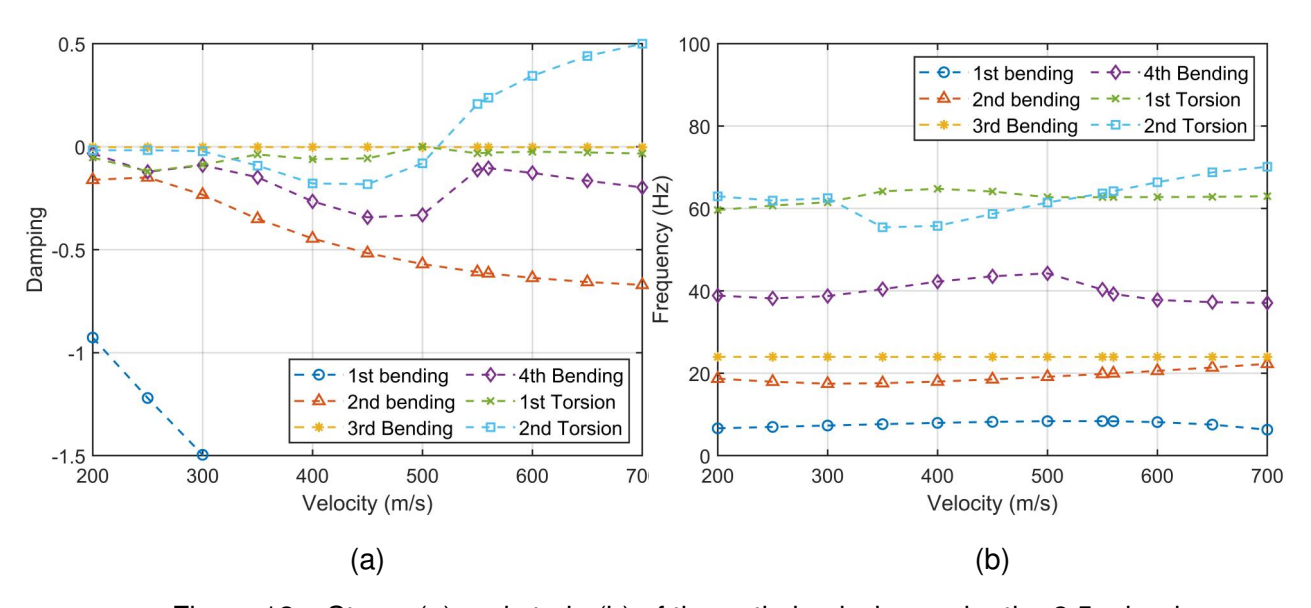


Figure 12 – Stress (a) and strain (b) of the optimized wing under the 2.5 g load.

4. Aeroelastic Tailoring and Optimization

An advantage of using composite skin and web panels in large aircraft wing design is that it allows to tailor laminate layups to modify wing stiffness, thereby optimizing its dynamic and flutter responses. At this stage, the laminate layups of the composite-optimized wing skin and web panels are tailored for aeroelastic performance. Each composite panel (upper and lower skin, front and rear spar web, and the middle web on the inner wing) has a distinct number of layers. The wing is divided into 7 sections, resulting in a total of 654 ply orientations to optimize. To save computational time, panel layups are optimized independently in different wing sections. As shown in Figure 13, wing section 2 significantly influences the wing flutter characteristics compared to section 1. Consequently, aeroelastic tailoring increases the flutter speed from 513.29 m/s to 624.62 m/s, a 21.69% improvement.

Table 5 – Aeroelastic tailoring settings for the optimized wing

Optimization objective
Optimization variables
Constraint

Maximize flutter speed
Composite laminate layups of different wingbox parts
with a total number of ply orientations: 654
None

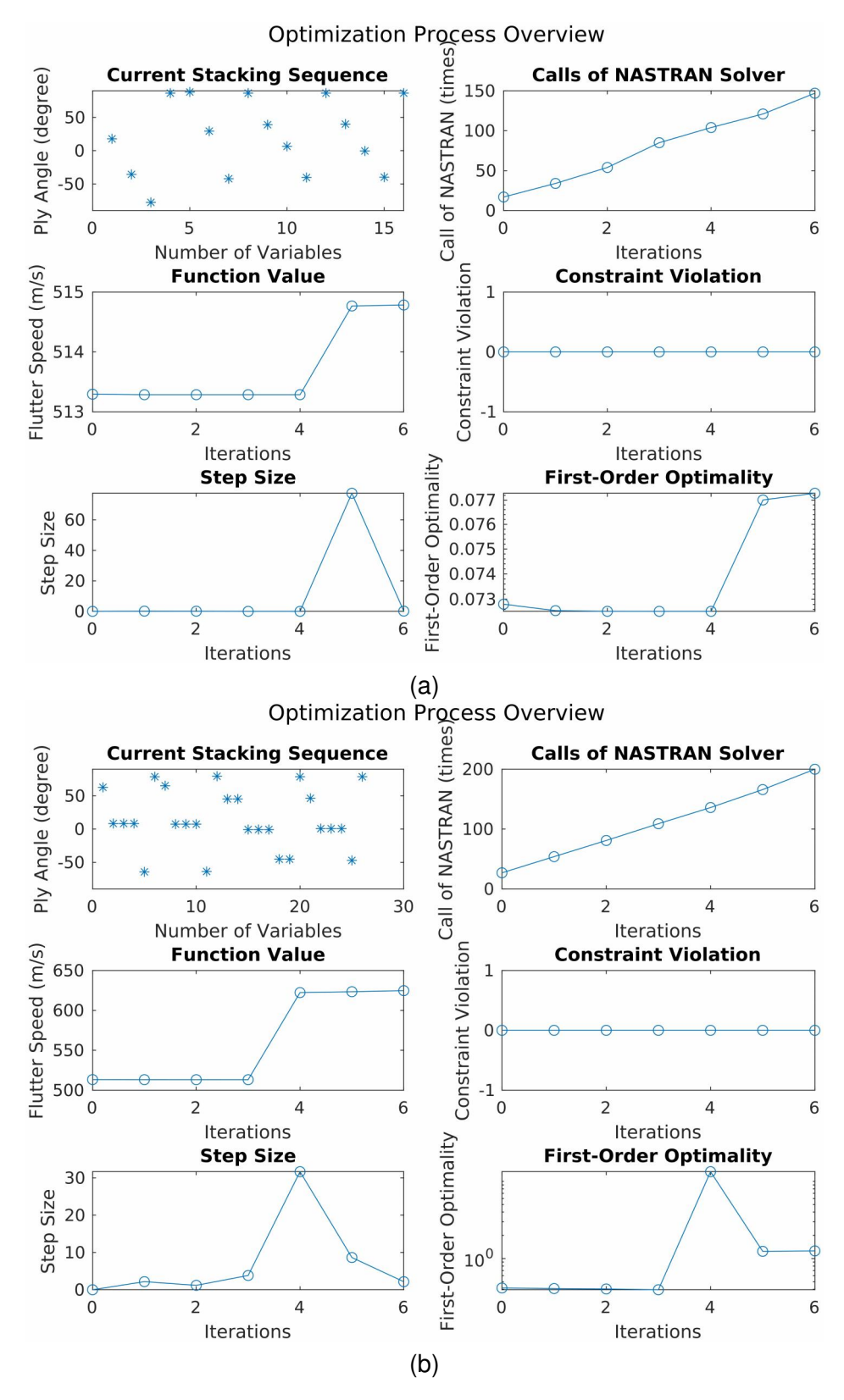


Figure 13 – Aeroelastic tailoring process for the optimized wing: (a) wing section 1 and (b) wing section 2.

5. PTWT Design and Analysis

5.1 PTWT Design

Key design parameters of PTWT, such as shaft location, torque spring stiffness, mass, and the location of centre of gravity, have been established in previous research [11, 12, 28]. Research by He et al. [10] indicates that while the mass and CG location of the PTWT minimally affect gust responses, they significantly influence the wing flutter characteristics. In the current study, the PTWT model remains the sizing of the optimized wing structure from the SLoT-SAIT stage. The PTWT replaces the original fixed wingtip (wing section 1) by modifying the wingtip segment constraints in the original FE model and has a length of 1.17 m. The shaft, serving as the PTWT front spar and spring supporter, is modeled as a bar element in the FE model, with sufficient bending and torsional stiffness. The torque spring is modeled using the CRLAS1 element. Figure 14 illustrates the PTWT design and optimization process for flutter suppression in this study, with torque spring stiffness and mass as the primary design variables. The spring stiffness is adjusted to determine the minimum stiffness required to achieve the desired flutter speed.

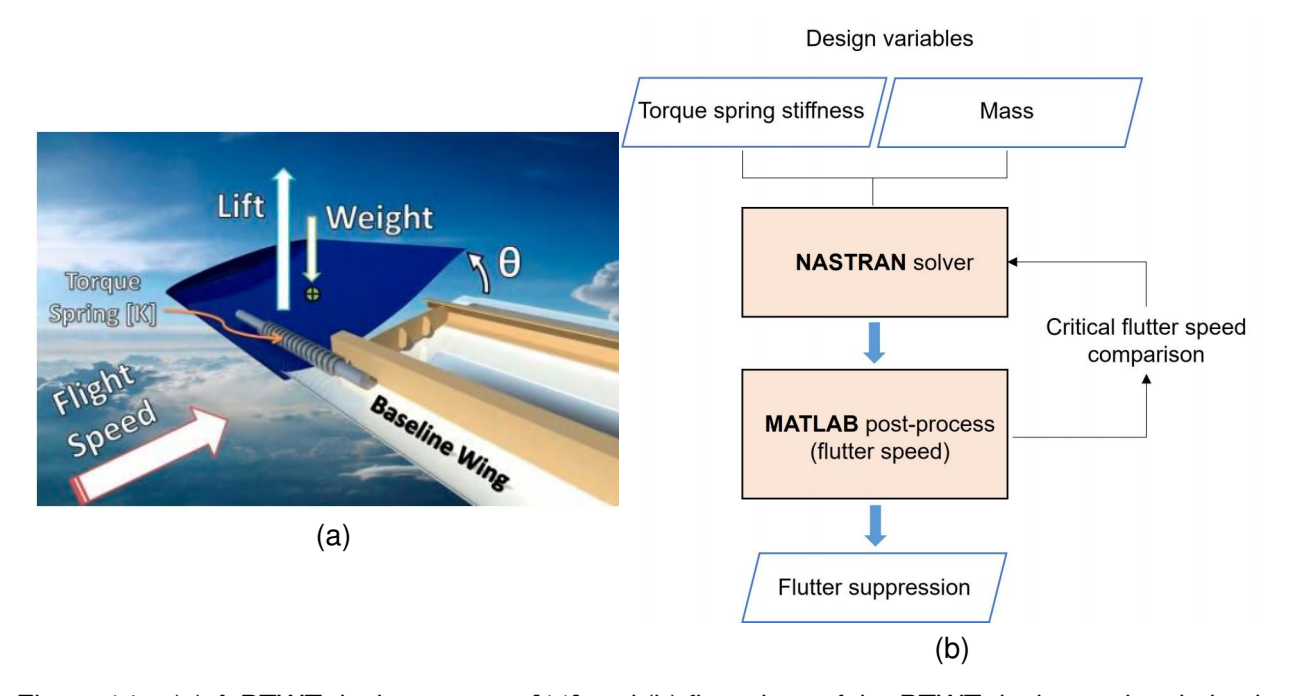


Figure 14 – (a) A PTWT design concept [11] and (b) flow chart of the PTWT design and optimization.

5.2 Influence on Flutter Characteristics

The flutter analysis of the wing with PTWT is performed over a spring stiffness range from 0.01 to $10 \ kNm/rad$. The PTWT weighs 138.34 kg without the shaft torque spring. A spring stiffness of 1 kNm/rad can be achieved using a steel helical spring with five coils, a coil diameter of 20 mm, and a spring diameter of 100 mm [11]. Figure 15 shows the variation in flutter speed across different stiffness and mass values. When the PTWT shaft has a spring stiffness of 0.5 kNm/rad and a total weight of 140.15 kg, the flutter speed exceeds $1.15V_D$, thus the PTET design can satisfy the aeroelastic stability requirement. Figure 16 presents the dominant modes for the flutter of the wing with PTWT, using a torque spring stiffness of 1 kNm/rad as an example. The PTWT mode (mode 1) results in a flutter speed of 216.07 m/s and a flutter frequency of 3.34 Hz. Notably, in modes 3 and 6, the PTWT and wing body behavior are coupled, leading to flutter speeds of 445.77 m/s (16 Hz) and 296.84 m/s (33.63 Hz), respectively. With the initial PTWT design implemented, future studies will investigate its gust alleviation capabilities, focusing on reducing gust responses in terms of bending moment at the wing root and wingtip deflection.

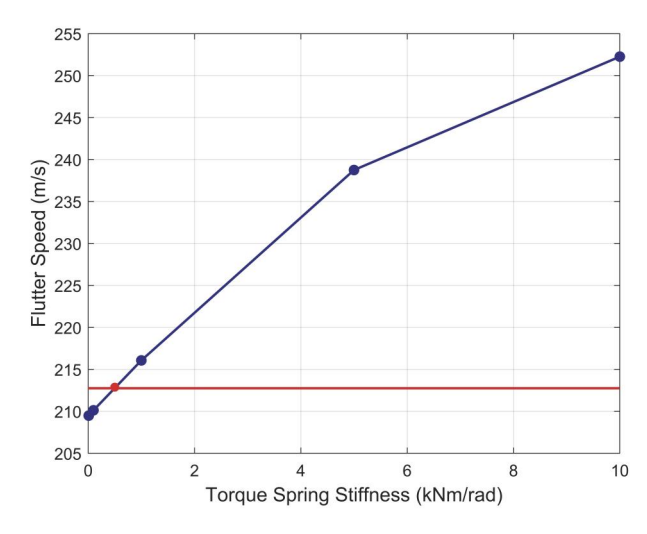


Figure 15 – Variation of flutter speed with the shaft torque spring stiffness.

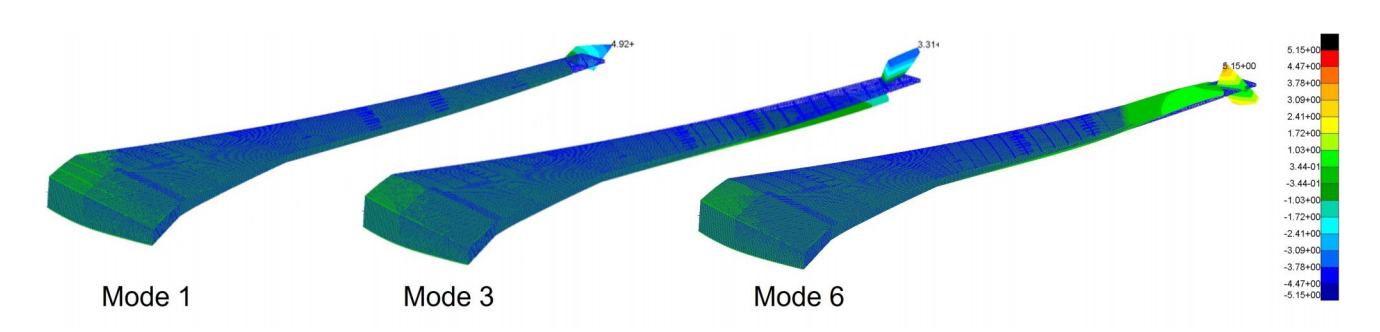


Figure 16 – Critical mode shapes of the PTWT with a spring stiffness of 1 kNm/rad.

6. Conclusion

This paper presents a flexible multi-fidelity toolset for optimizing a composite wing for a large aircraft, focusing on weight reduction and flutter speed improvement. The toolset integrates medium-fidelity structural analysis and aeroelastic tailoring through the in-house SLoT-SAIT programs, high-fidelity FEM-based optimization using the NASTRAN solver and MATLAB optimizer, and the implementation of a PTWT design for enhanced aeroelastic characteristics. The SLoT-SAIT programs have been found to be efficient for designing a composite wing structure with minimum weight while meeting multiple constraints, including strength and flutter. By optimizing the ply thickness and arranging plies according to fiber orientations for each wingbox section in skin-stringer panels, the design variables are reduced and computing time is saved. Results show significant weight savings and improved flutter speed could be achieved through tailoring skin laminate thickness and optimizing the ply stacking sequences. The toolset allows for rapid and automatic wing structural sizing and flutter predictions within minutes, ensuring accuracy comparable to the detailed analysis of high-fidelity FEMs. The flexibility of the toolset allows for adaptation to different variables and cases, with the potential for more functions like PTWT design. This optimization framework demonstrates its advantages and flexibility, enabling efficient airframe layout determination for new configurations and architectures from the MDO perspective in overall aircraft designs.

7. Contact Author Email Address

y.pan@cranfield.ac.uk

8. Copyright Statement

The authors confirm that they, and/or their company or organisation, hold copyright on all of the original material included in this paper. The authors also confirm that they have obtained permission, from the copyright holder of any third party material included in this paper, to publish it as part of their paper. The authors confirm that

they give permission, or have obtained permission from the copyright holder of this paper, for the publication and distribution of this paper as part of the ICAS proceedings or as individual off-prints from the proceedings.

Acknowledgement

This research is funded by the Out of Cycle NExt generation highly efficient air transport (ONEheart) project funded through the UK Research and Innovation. The authors would like to thanks for the support and cooperation from the Airbus OperationsLimited, United Kingdom.

References

- [1] Collier F, Thomas R, Burley C, Nickol C, Lee C M, and Tong M. Environmentally responsible aviation Real solutions for environmental challenges facing aviation. *27th Congr. Int. Counc. Aeronaut. Sci. 2010, ICAS 2010,* 1:300–315, 2010.
- [2] Bezos-O'Connor G M, Mangelsdorf M F, Maliska H A, Washburn A E, and Wahls R A. Fuel efficiencies through airframe improvements. *3rd AIAA Atmos. Sp. Environ. Conf.*, pages 1–13, 2011.
- [3] Wunderlich T F, Dähne S, Reimer L, and Schuster A. Global aero-structural design optimization of composite wings with active manoeuvre load alleviation. *CEAS Aeronaut. J.*, 13(3):639–662, jul 2022.
- [4] Kenway G K W, Kennedy G J, and Martins J R R A. Scalable parallel approach for high-fidelity steady-state aeroelastic analysis and adjoint derivative computations. *AIAA J.*, 52(5):935–951, 2014.
- [5] Guo S, Cheng W, and Cui D. Aeroelastic tailoring of composite wing structures by laminate layup optimization. *AIAA J*, 44:3146–3150, 12 2006.
- [6] Guo S. Aeroelastic optimization of an aerobatic aircraft wing structure. *Aerospace Science and Technology*, 11(5):396–404, 2007.
- [7] Yu Y, Wang Z, and Guo S. Efficient method for aeroelastic tailoring of composite wing to minimize gust response. *Int. J. Aerosp. Eng.*, 2017, 2017.
- [8] Alam M, Hromcik M, and Hanis T. Active gust load alleviation system for flexible aircraft: mixed feedforward/feedback approach. *Aerospace Science and Technology*, 41:122–133, 2 2015.
- [9] Jonathan C, Simon M, Otto S, and Gareth V. Optimization of a scaled sensorcraft model with passive gust alleviation. In *12th AIAA/ISSMO Multidisciplinary Analysis and Optimization Conference*, page 5875, 2008.
- [10] He S, Guo S, Liu Y, and Luo W. Passive gust alleviation of a flying-wing aircraft by analysis and wind-tunnel test of a scaled model in dynamic similarity. *Aerospace Science and Technology*, 113:106689, 2021.
- [11] Guo S, De Los Monteros J E, and Liu Y. Gust alleviation of a large aircraft with a passive twist wingtip. *Aerospace*, 2(2):135–154, 2015.
- [12] Guo S, Jing Z W, Li H, Lei W T, and He Y Y. Gust response and body freedom flutter of a flying-wing aircraft with a passive gust alleviation device. *Aerospace Science and Technology*, 70:277–285, 2017.
- [13] NASA common research model [online database]. http://commonresearchmodel.larc.nasa.gov/. Accessed: 11 Dec. 2023.
- [14] Vassberg J., Dehaan M., Rivers M., and Wahls R. Development of a common research model for applied CFD validation studies. In *26th AIAA Applied Aerodynamics Conference*, H, Hawaii, 2008.
- [15] John V. A unified baseline grid about the common research model wing/body for the fifth AIAA CFD drag prediction workshop (invited). In *29th AIAA Applied Aerodynamics Conference*, H, Hawaii, 2011.
- [16] Lyu Z and Martins J R R A. Aerodynamic design optimization studies of a blended-wing-body aircraft. *Journal of Aircraft*, 51(5):1604–1617, 2014.
- [17] Hue D, Sartor F, Petropoulos I, and Fournis C. DPW-7: steady and unsteady computations of the common research model at different reynolds numbers. *Journal of Aircraft*, 60(6):1857–1871, 2023.
- [18] Kenway G, Kennedy G, and Martins J R R A. Aerostructural optimization of the common research model configuration. In *15th AIAA/ISSMO Multidisciplinary Analysis and Optimization Conference*, Atlanta, GA, 2014.
- [19] Klimmek T. Parametric set-up of a structural model for fermat configuration for aeroelastic and loads analysis. In *ASDJournal*, volume 3, pages 31–49, 2014.
- [20] Kenway G K W and Martins J R R A. Multipoint high-fidelity aerostructural optimization of a transport aircraft configuration. *Journal of Aircraft*, 51(1):144–160, 2014.
- [21] Common Research Model (CRM) wingbox finite element models. https://commonresearchmodel.larc.nasa.gov/wp-content/uploads/sites/7/2014/02/CRM_wingboxFEM_description_1.pdf. Accessed: 11 Dec 2023.

- [22] 7th AIAA CFD drag prediction workshop [online database]. https://aiaa-dpw.larc.nasa.gov/Workshop7/DPW7-geom.html. Accessed: 11 Dec. 2023.
- [23] Spinelli A and Kipouros T. PDOPT: a python library for probabilistic design space exploration and optimisation. *Journal of Open Source Software*, 9(95):6110, 2024.
- [24] MATLAB. 'fminunc'. MathWorks. https://www.mathworks.com/help/optim/ug/fminunc.html. Accessed: 11 Dec 2023.
- [25] Baker A A. Composite materials for aircraft structures. AIAA, 2004.
- [26] Computer program for estimation of spanwise loading of wings with camber and twist in subsonic attached flow. Lifting-surface theory. https://www.esdu.com/cgi-bin/ps.plsess=cranfield5_1240514170720hrx&t=t_and_c&p=university&fwd_t=doc&fwd_p=esdu_95010c. Accessed: 14 May 2024.
- [27] Bret K S and Steven J M. Uncertainty quantification of the FUN3D-predicted NASA CRM flutter boundary. In *SciTech Forum*, number NF1676L-24499, 2017.
- [28] Guo S, Li D, and Sensburg O. Optimal design of a passive gust alleviation device for a flying wing aircraft. 12th AIAA Aviation Technology, Integration, and Operations (ATIO) Conference and 14th AIAA/ISSMO Multidisciplinary Analysis and Optimization Conference.